Supporting Information for: Role of molecular disorder on the reactivity of RDX

Michael Sakano, Brenden Hamilton, Md Mahbubul Islam, Alejandro Strachan*

School of Materials Engineering and Birck Nanotechnology Center, Purdue University, West Lafayette, Indiana, 47907, United States

*Corresponding author: strachan@purdue.edu

This supplementary material contains information regarding comparisons between crystal and amorphous systems from homogeneous thermal decomposition, hot spot gradients, and thermal conductivity measurements. Differences in materials characterization techniques like structure factor suggest that our created an amorphous structure is distinguishable from its crystalline counterpart. In terms of differences in reactivity, we compared their activation energies under isothermal conditions and looked into the thermodynamics in explaining similarities between our compressed lattice parameter samples. From the chemical species analysis, we note insignificant differences in the dissociation of RDX under homogeneous decomposition simulations between our four samples. We iterate that modifying the bond cutoff does not display much differences in the major intermediate NO_2 and product N_2. We also address similarities in chemistry in our thermal hot spot simulations between crystal and amorphous experimental density samples, though the amorphous reaction zone propagates at a slightly faster radial velocity. Finally, we compare differences in the thermal conductivity in our non-reactive simulations and our results are in good agreement with prior experiments and other similar simulations.

Structural Comparisons

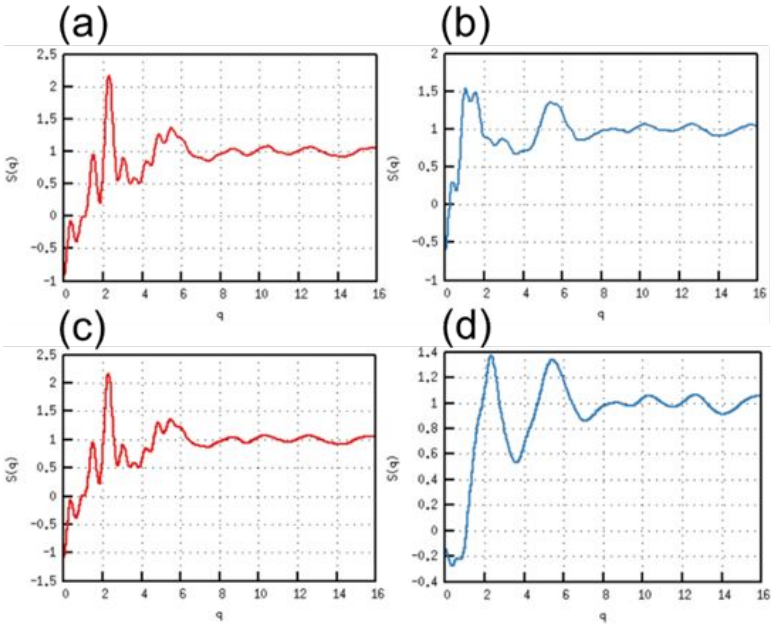

Fig S1: Structure factor calculations for (a) experimental crystal, (b) experimental amorphous, (c) compressed crystal, and (d) compressed amorphous 3 x 3 x 3 RDX unit cells structures.

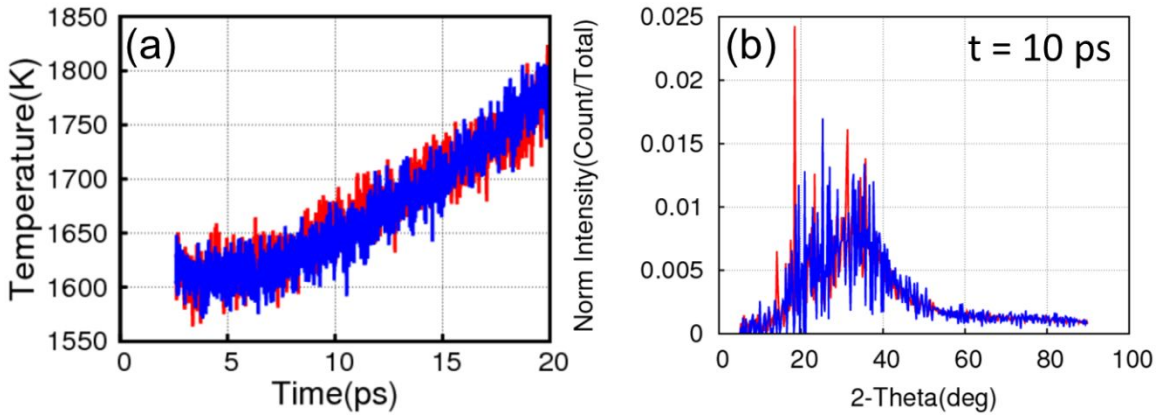

Fig S2: (a) Initial portion of temperature profile for one of the samples of crystal and amorphous 3 x 3 x 3 RDX structures with compressed lattice parameters, (b) XRD snapshot 10 ps after ramping to 1600 K.

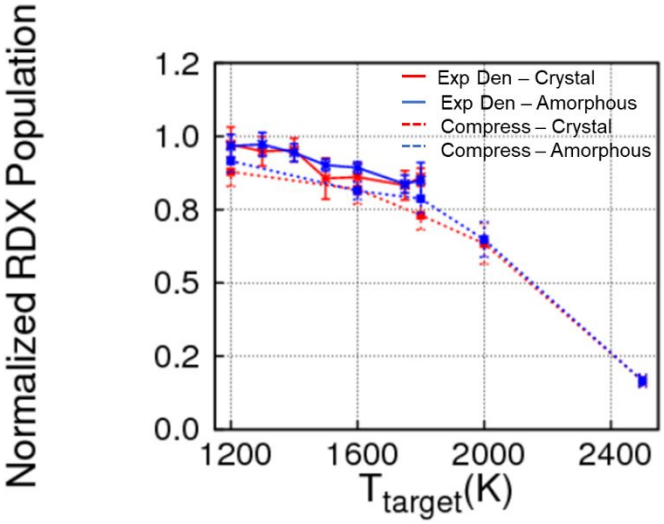

Fig S3: Normalized RDX population following the completion of endothermic processes as a function of the ramped target temperature. Similar values between structures and densities for temperatures between 1200 K and 1800 K.

Thermal Decomposition Chemistry

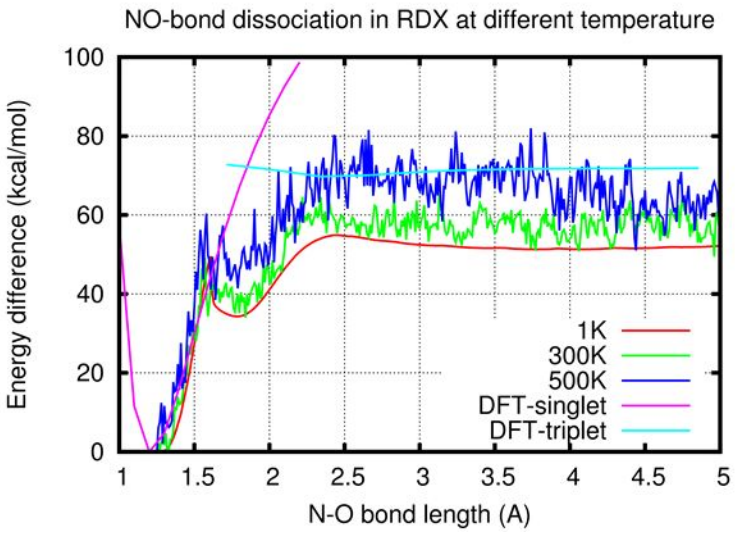

Fig S4: Dissociation curves for N-O in the RDX crystal. ReaxFF underpredicts dissociation energy compared to DFT. At elevated temperatures, kink in the bond dissociation profile around 1.6 Angstroms becomes less significant.

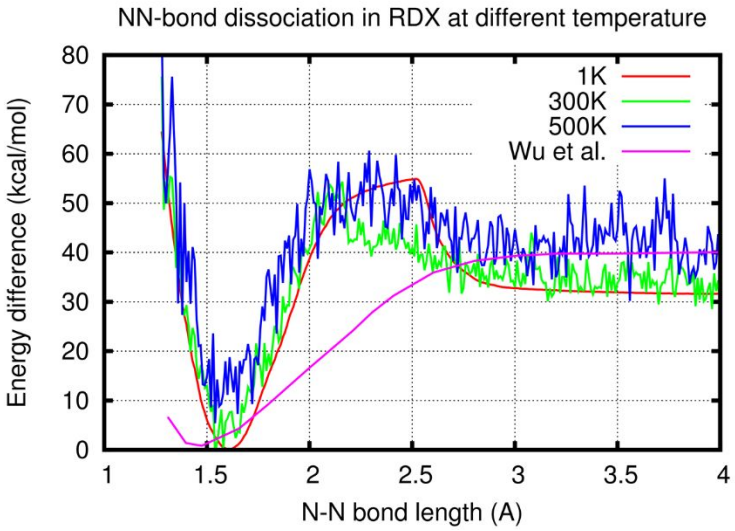

Fig S5: Dissociation curves for N-N in RDX crystal. DFT reference by Wu and Fried.[1]

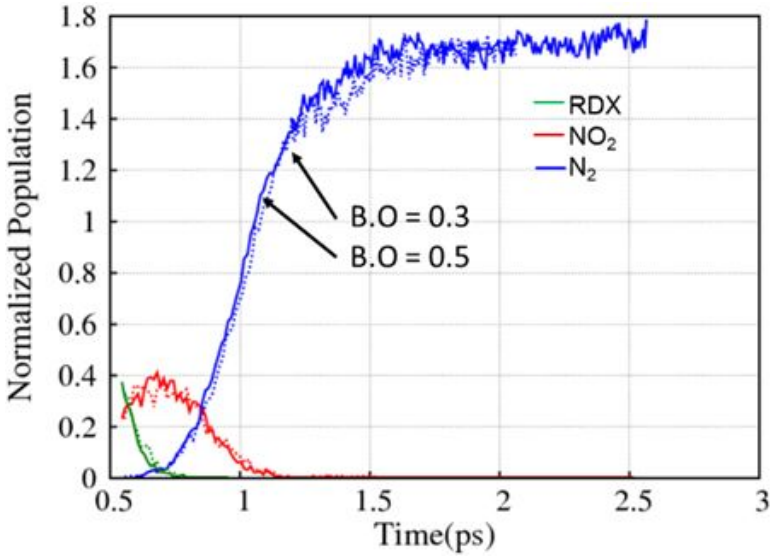

Fig S6: Species distribution for RDX, NO_2, and N_2 at 2500 K. Similarities between bond order indicates insignificant difference in formation of species.

Hot spot Chemistry

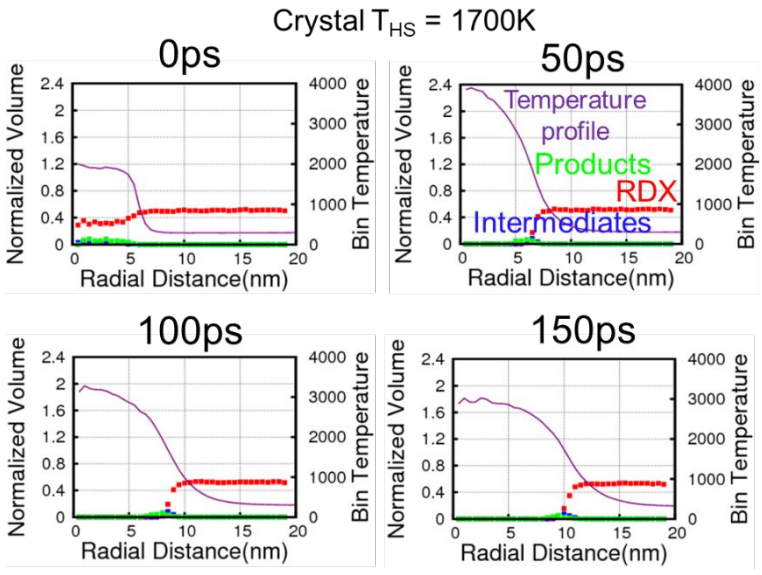

Fig S7: Magnitude of binned intermediates and products as a function of radial distance for 1700 K hot spots in a crystal sample at experimental density.

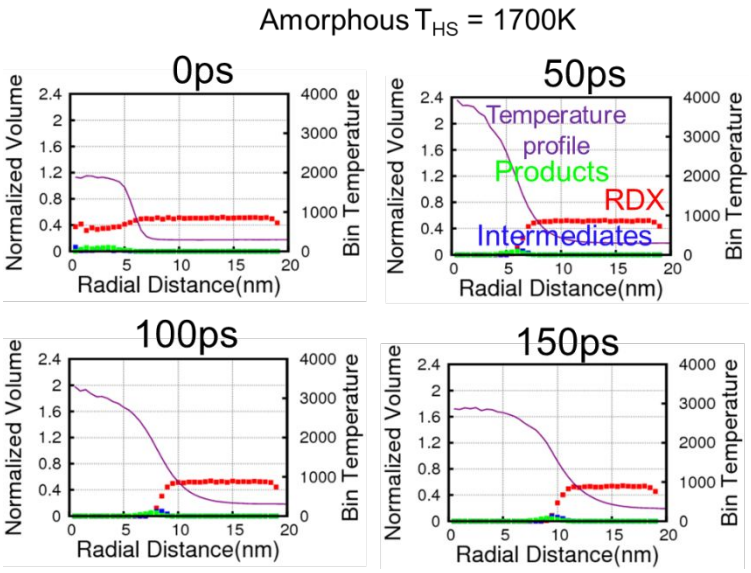

Fig S8: Magnitude of binned intermediates and products as a function of radial distance for 1700 K hot spots in an amorphous sample at experimental density.

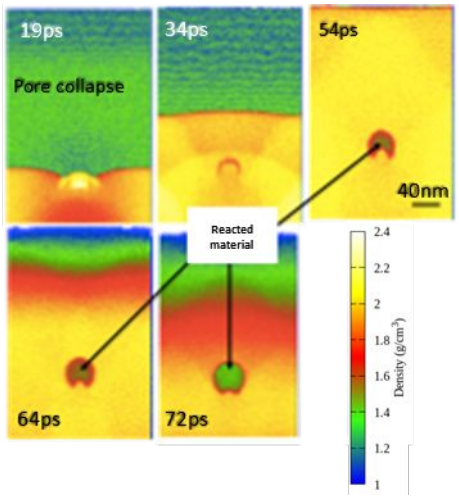

Fig. S9: Density maps during the collapse of a pore with diameter of 40 nm. Initial decrease in density only when intermediate chemistry begins.

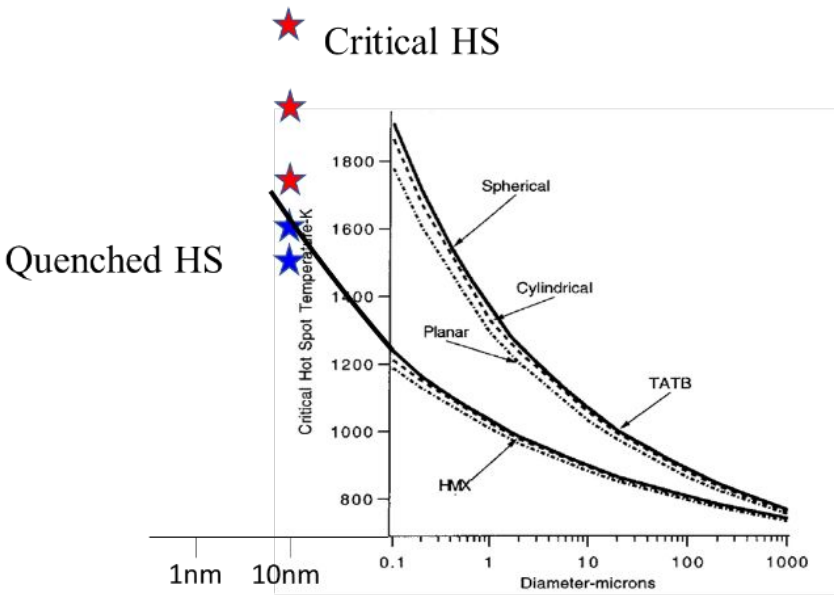

Figure S10: Critical (red stars) and non-critical (blue stars) hot spot temperatures for 10 nm hot spots in good agreement with the Tarver model.[2]

Thermal Conductivity

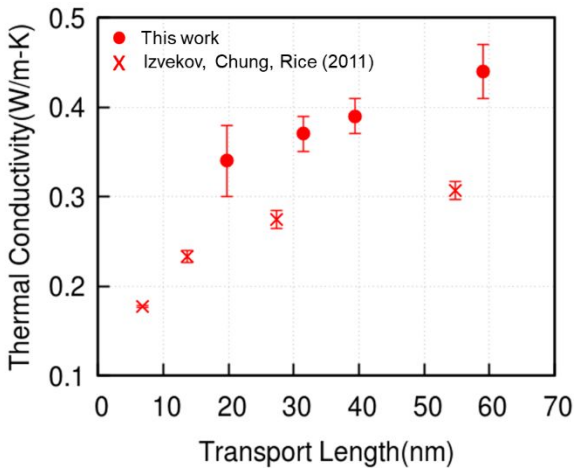

Figure S11: Thermal conductivity as it follows transport length for this work, as well as data by Izvekov, Chung, and Rice[3] showing good agreement in nanoscale heat transport. Transport calculated at 300 K in the [100] lattice direction.

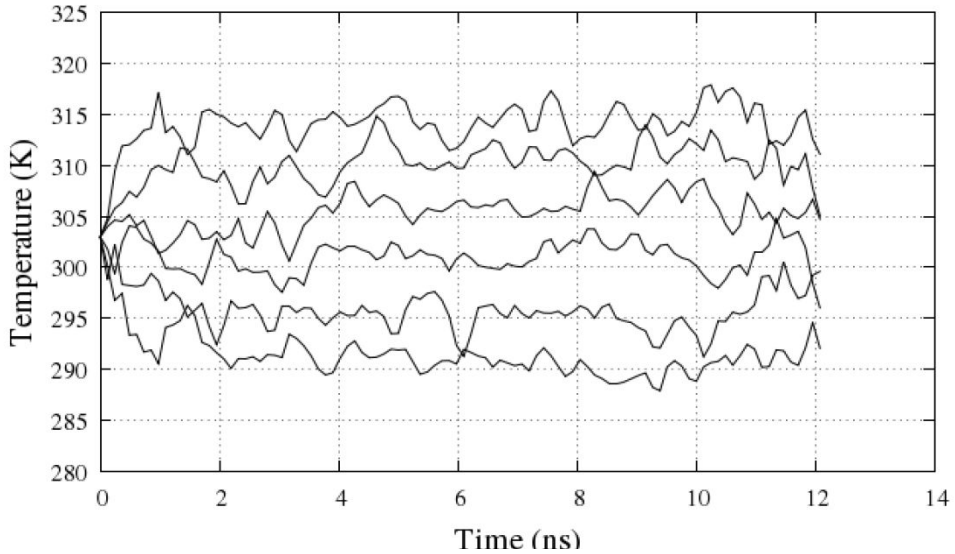

Figure S12: Time evolution of thermal gradient for crystalline sample, 39nm in length. Each line represents a separate bin for local temperature analysis.

Table S1: Thermodynamic Comparison between experimental and compressed lattice parameter systems

System	PE (kcal/mol-molecule) 300 K	PE (kcal/mol-molecule) 1200 K	Exothermicity (kcal/mol-molecule)
Crystal $\rho = 1.86$ g/cm^3	-1927.6	-1865.5	185
Amorphous $\rho = 1.86$ g/cm^3	-1921.8	-1859.1	187
Crystal $\rho = 2.15$ g/cm^3	-1904.8	-1843.7	162
Amorphous $\rho = 2.15$ g/cm^3	-1897.2	-1835.0	165

Table S2: Conductivity data for bulk extrapolation

Transport Length (nm)	Crystalline Conductivity (W/m-K)	Amorphous Conductivity (W/m-K)
19	.347 + .046	.347 + .037
32	.370 + .023	.357 + .011
39	.392 + .024	.369 + .021
59	.450 + .035	.399 + .030
Bulk (κ_∞)	.594 W/m-K	.459 W/m-K
MFP	9.71 nm	4.62 nm

References

(1) Wu, C. J.; Fried, L. E. Ab Initio Study of RDX Decomposition Mechanisms. *J. Phys. Chem. A* **1997**, *101* (46), 8675–8679.

(2) Tarver, C. M.; Chidester, S. K.; Nichols, A. L. Critical Conditions for Impact- and Shock-Induced Hot Spots in Solid Explosives. *J. Phys. Chem.* **1996**, *100* (14), 5794–5799.

(3) Izvekov, S.; Chung, P. W.; Rice, B. M. Non-Equilibrium Molecular Dynamics Simulation Study of Heat Transport in Hexahydro-1,3,5-Trinitro-s-Triazine (RDX). *Int. J. Heat Mass Transf.* **2011**, *54* (25), 5623–5632.